ELSEVIER

Journal of Molecular Graphics and Modelling 20 (2002) 359–371

Journal of Molecular Graphics and Modelling

www.elsevier.com/locate/JMGM

Differential binding mode of diverse cyclooxygenase inhibitors

Oriol Llorens [a], Juan J. Perez [a,*], Albert Palomer [c], David Mauleon [b]

[a] *Department of d'Enginyeria Química, UPC, ETSEIB, Av. Diagonal, 647, 08028 Barcelona, Spain*
[b] *Laboratorios Menarini, Alfonso XII, 587, 08912 Badalona, Spain*
[c] *Ferrer Internacional S.A., Juan de Sada, 32, 08028 Barcelona, Spain*

Received 21 April 2001; received in revised form 26 October 2001; accepted 6 November 2001

Abstract

Non-steroideal anti-inflammatory drugs (NSAIDs) are competitive inhibitors of cyclooxygenase (COX), the enzyme that mediates biosynthesis of prostaglandins and thromboxanes from arachidonic acid. There are at least two different isoforms of the enzyme known as COX-1 and -2. Site directed mutagenesis studies suggest that non-selective COX inhibitors of diverse chemical families exhibit differential binding modes to the two isozymes. These results cannot clearly be explained from the sole analysis of the crystal structures of COX available from X-ray diffraction studies. With the aim to elucidate the structural features governing the differential inhibitory binding behavior of these inhibitors, molecular modeling studies were undertaken to generate atomic models compatible with the experimental data available. Accordingly, docking of different COX inhibitors, including selective and non-selective ligands: rofecoxib, ketoprofen, suprofen, carprofen, zomepirac, indomethacin, diclofenac and meclofenamic acid were undertaken using the AMBER program. The results of the present study provide new insights into a better understanding of the differential binding mode of diverse families of COX inhibitors, and are expected to contribute to the design of new selective compounds.

Keywords: Cyclooxygenase docking; NSAIDs; Molecular modeling; AMBER

1. Introduction

Cyclooxygenase (COX) is an endogenous enzyme that catalyzes the first committed step in the conversion of arachidonic acid into prostaglandins and thromboxanes. These molecules mediate different important functions in the gastric, renal and hematic systems and regulate different processes like inflammation and body temperature [1,2]. COX is competitively inhibited by a group of drugs known as non-steroideal anti-inflammatory drugs (NSAIDs). Their action results in the anti-inflammatory, analgesic, antipyretic and antithrombotic activity exhibited by this group of molecules. Members of this group include well known therapeutic agents like aspirin, diclofenac, ibuprofen, indomethacin or naproxen [3]. Spite of their beneficial action, their activity is associated with deleterious side effects, and continuous administration of these drugs leads to nefrotoxicity and gastric ulcerations [4,5]. Consequently, new NSAIDs without side effects are necessary for safer treatments.

A key discovery in the search of novel anti-inflammatory therapeutic agents lacking the deleterious side effects exhibited by traditional NSAIDs, came from the characterization and isolation of two different COX isoforms, known as COX-1 and -2. Interestingly, although the two enzymes catalyze the same chemical transformation, both isoforms are subject to a different expression regulation. Thus, while COX-1 is constitutively expressed and it is involved in the synthesis and supply of the necessary arachidonic acid metabolites for a maintenance of gastric and renal functions as well as for an adequate vascular homeostasis, COX-2 is expressed only after an inflammatory stimulus, releasing metabolites that are used to induce inflammation and pain [6–8]. This discovery, together with the fact that traditional NSAIDs show very little selectivity for COX-2, prompted to suggest [9] that the therapeutic anti-inflammatory action of NSAIDs is produced by inhibition of COX-2, while the unwanted side effects arise from inhibition of COX-1 activity.

Accordingly, a great deal of interest has been devoted in recent years to the discovery of selective COX-2 inhibitors. As a result of these investigations, the two first COX-2 selective inhibitors: celecoxib [10] and rofecoxib [11] are already in clinical use. These new structures exhibit an increased selectivity for COX-2 and little side effects [12]. Their success as therapeutic agents, justifies the enormous expectations and interest in the discovery of new leads.

The process of designing novel selective COX inhibitors requires to characterize structural differences between the two isozymes. Crystal structures of both COX-1 and -2 with different ligands docked in their active site were solved using

* Corresponding author. Tel.: +34-934016685; fax: +34-934017150.
E-mail address: juanje@eq.upc.es (J.J. Perez).

1093-3263/02/$ – see front matter
PII: S1093-3263(01)00135-8

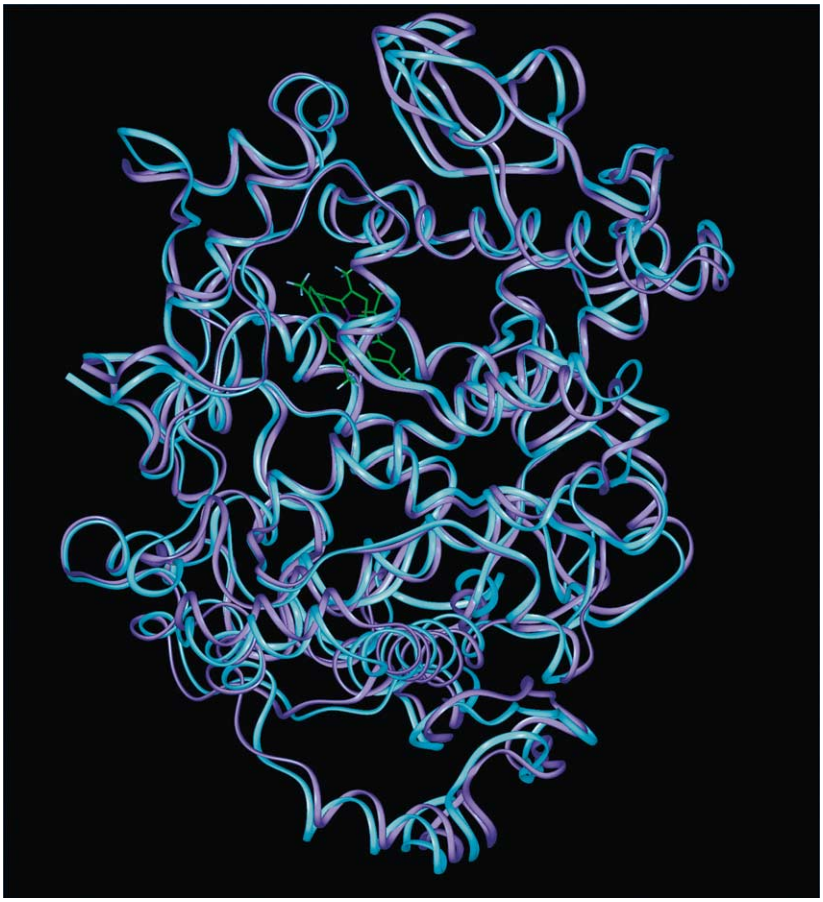

Fig. 1. Superposition of the 3D structures of COX-1 (in light blue) and COX-2 (in dark blue). The heme group is shown in green.

X-ray diffraction methods and are nowadays available in the literature [13–17]. Overall differences between the two structures are small as illustrated in Fig. 1, and superposition of the 3D structures yields a rmsd of 0.9 Å computed from the α-carbons of the two isozymes. The 3D structure of the two enzymes exhibit three common domains [18]: (a) the region between residues 34 and 72 at the N-terminus, known as the epidermal growth factor domain (residue numbering refers to COX-1 throughout the present work); (b) the membrane binding domain, between residues 73 and 116, with numerous hydrophobic residues involved in its attachment to the cell membrane; (c) the C-terminus, a large domain containing the COX active site on top of a hydrophobic channel connecting it to the membrane domain.

The two enzymes are highly homologous, exhibiting a 61% sequence identity that achieves a 87% when only the subset of residues located in the COX active site are compared. Alignment of the two sequences reveals the insertion of a proline residue after Ile^{106} in COX-2. However, since this residue is located on a loop of the membrane domain, the insertion does not perturb the overall 3D structure of the enzyme [19]. The largest number of non-conserved residues are located at the membrane domain. However, most of the substitutions preserve their hydrophobic profile, consistent with its putative role as membrane anchoring domain of the enzyme.

Inhibition of the enzyme at the molecular level is mediated through the blockade of arachidonic acid to access the COX active site. Accordingly, a detailed analysis of this binding site provides keys for designing novel inhibitors with increased affinity and selectivity. Inspection of the COX active site reveals three differential regions, shown in Fig. 2: (a) a hydrophobic pocket beneath the heme group, defined by the residues Tyr^{385}, Trp^{387}, Phe^{518}, Ala^{201}, Tyr^{248} and Leu^{352}; (b) the mouth of the active site, with three hydrophilic residues flanking its entrance: Arg^{120}, Glu^{524}, Tyr^{355}, and arranged to form a hydrogen bond network; (c) a side pocket, larger in COX-2, defined by several conserved residues including His^{90} and the non-conserved residues His/Arg^{513} and Ile/Val^{523}.

In spite of the insight provided from the comparative analysis of the structures of the two isozymes solved by X-ray diffraction studies, crystal structures alone cannot provide a complete explanation of different information obtained from diverse mutagenesis studies, strongly pointing that NSAIDs exhibit differential docking modes in the COX active site [20–29]. In this conditions, modeling studies are required in order to construct molecular models that incorporate all experimental evidence reported. These models are necessary to obtain a consistent, more precise picture of the enzyme–inhibitor recognition step at the atomic level and

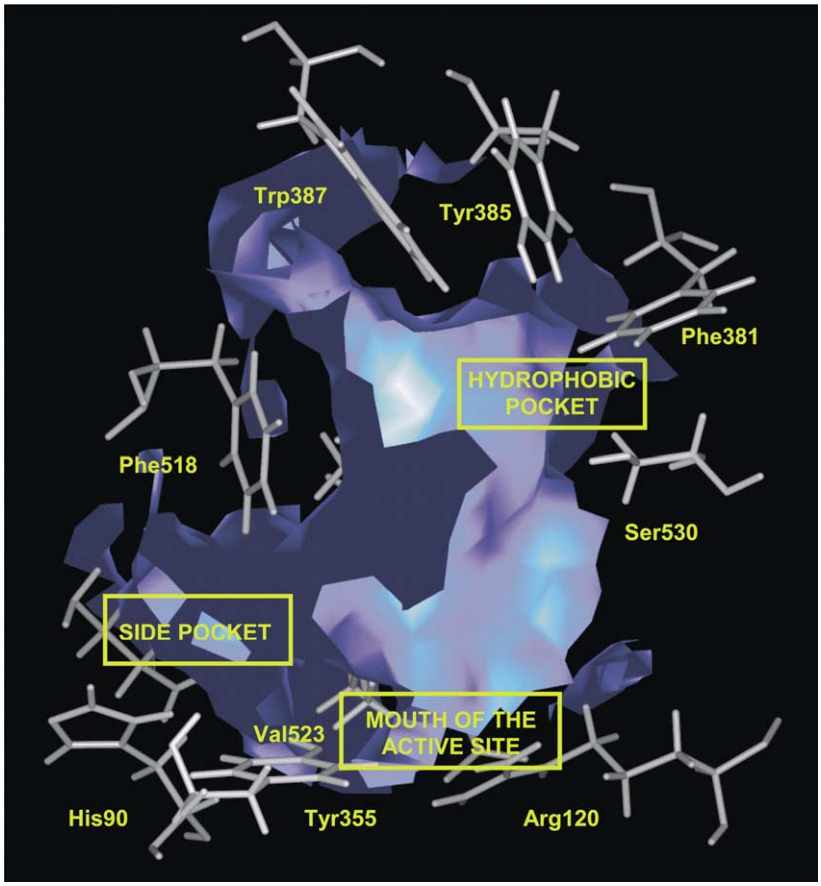

Fig. 2. Boundary surface defining the cyclooxygenase binding pocket computed on the COX-1 isozyme with GRID. Different regions of the pocket as well as the side chains of key residues are explicitly shown.

furthermore, provide new insights that can be used to design novel therapeutic agents.

The purpose of the present work is to construct molecular models of different inhibitor–enzyme complexes based on the available structural information of COX inhibition, that incorporate the findings of different site mutagenesis experiments. Specifically, the present work reports the results of a series of docking studies of a selective (rofecoxib) and diverse non-selective (ketoprofen, suprofen, carprofen, zomepirac, indomethacin, diclofenac and meclofenamic acid) COX inhibitors (see in Fig. 3 for structures), into the COX active site of the two isoforms. This information is important to characterize the structural features of the different families of NSAIDs relevant for their recognition with each of the two isozymes as well as provide new insights for the design of novel more potent selective inhibitors.

2. Methods

Crystal structures of the enzymes COX-1 (entry 1PRH) [13] and COX-2 (entry 3PGH) [14] with flurbiprofen bound to the COX binding site were obtained from the Brookhaven Data Bank [30]. Coordinates of the ligand were removed from the files and the structures of the two enzymes were energy minimized in vacuo with a distance dependent dielectric constant 4*r*, using a conjugated gradient minimization algorithm implemented in the AMBER program [31], until the rmsd of two successive iterations was <0.001 Å. All the molecular mechanics calculations reported in the present work, were performed using the all-atom parm91 force field set of parameters [32]. Structures of the inhibitors studied in the present work were constructed using the PREP module of AMBER. Force field parameters were taken from the standard parm91 set and partial atomic charges were generated by fitting the molecular electrostatic potential, computed with a STO-3G basis set using the GAUSSIAN94 suite of programs [33]. Ligands were manually docked into the COX binding pocket of COX-1 and -2, guided by the crystal structures of structurally related inhibitors [13–16], site directed mutagenesis studies and GRID calculations [34,35] performed on the COX binding site of the enzyme with diverse probes. Complexes generated were energy optimized in vacuo, with a distance dependent dielectric constant of 4*r*, using a conjugated gradient minimization algorithm until the rmsd of two successive iterations was <0.001 Å. Display and examination of the models was carried out using the InsightII program [36].

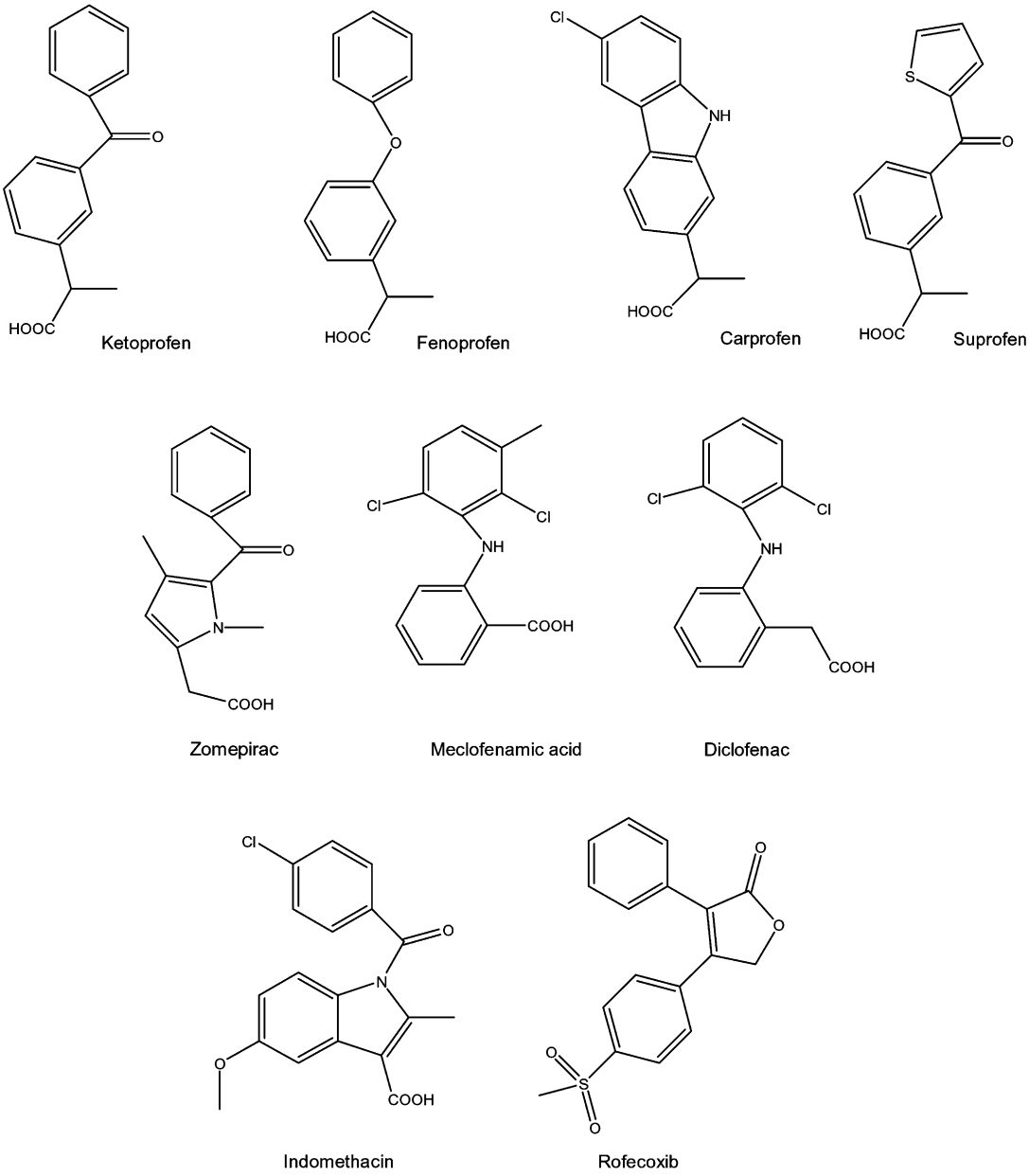

Fig. 3. Chemical structures of the different COX inhibitors selected for the present study.

3. Results

Results of the computations performed in the present work are described below and are organized by families according to the chemical structures of the different inhibitors studied.

3.1. Phenyl acetic acids: ketoprofen, carprofen, fenoprofen and suprofen

Members of this group of NSAIDs are characterized by a 2-methylphenylacetic scaffold with an aromatic moiety attached in *meta* (see Fig. 3). Specifically, the different members of this family selected for the present study exhibit the following aromatic rings: a benzoyl moiety in the case of ketoprofen, a phenoxy moiety in fenoprofen, a thienylcarbonyl moiety in suprofen. Carprofen is a tricyclic molecule that can be understood as an 6-chloroindole moiety fused to the phenyl acetic ring. These compounds are non-selective NSAIDs and their relative inhibitory potency in COX-1 follows the order [37]: ketoprofen > suprofen > fenoprofen > carprofen. Interestingly, the *S*-enantiomers of these ligands are more potent than the corresponding *R*-stereoisomers in all the cases.

Manual docking of the inhibitors using InsightII [36] was performed by placing the different ligands in the COX active site of the two isozymes, using the crystal structures of the

structurally related inhibitor flurbiprofen as template [13,14] and taking into consideration the mutagenesis studies available. For this purpose, several molecular interactions were considered to be responsible for the observed affinities (see Fig. 4): (i) a hydrogen bond interaction between the ligand carboxylate moiety and the guanidinium moiety of the Arg^{120} side chain; (ii) a hydrogen bond interaction between the heteroatom bridging the two aromatic rings of the ligand and the side chain of Ser^{530} and (iii) a hydrophobic interaction between the aromatic moiety common to the different ligands and the aromatic pocket formed by the side chains of Tyr^{385}, Trp^{387}, Phe^{518}, Ala^{201}, Tyr^{348} and Leu^{352}.

After energy minimization, complexes were inspected to check whether the different ligand–enzyme key interactions were conserved during the minimization process. It is important to note that, due to the multiple minima problem associated with the ligand–enzyme potential energy surface, several docking attempts had to be undertaken for each ligand. Those complexes conserving all key interactions after minimization, were considered representative models of the corresponding ligand. It was found that all the compounds, but fenoprofen, preserved all key interactions after optimization. As illustration, Fig. 4 shows the optimized structure of ketoprofen docked into the COX-1 active site. In the fenoprofen complex, the interaction between the ligand and the Ser^{530} side chain could not be preserved and in the final structure the ligand appears displaced from its initial position, with a structure where the ether oxygen and the hydroxyl moiety of the Ser^{530} side chain lie at a long distance from each other. This is likely due to the higher rotational freedom exhibited by the phenyl ring of this ligand, and corroborated by the observation that after different attempts of docking fenoprofen to the active site, the ether oxygen was found in all the cases pointing outwards the Ser^{530}.

Analysis of these complexes reveals some ligand key structural features that appear relevant for their inhibitory activity. Thus, present results suggest that the dihedral angle between the two aromatic rings around 30° is important for an efficient ligand–receptor interaction. This explains the poorer affinity exhibited by carprofen, where the two aromatic rings are constrained to be in the same plane. Another structural feature regards the size of the aromatic moiety. A phenyl moiety fills better the hydrophobic pocket next to Tyr^{385} providing a stronger interaction with the enzyme, as supported by the lower potency exhibited by suprofen as compared with that of ketoprofen. Present models also suggest that the lower affinity of fenoprofen can be explained as a consequence of the two effects. On the one hand, the larger rotational freedom exhibited by the molecule through the ether moiety in comparison with the other ligands of the same family and on the other, its poorer hydrogen bond acceptor capability as compared to a carbonyl oxygen, which results in a loss of a key interaction with the side chain of Ser^{530}.

The observed preference of the *S*-enantiomers for COX, as deduced from the structure-activity studies of this family of compounds can also be explained with the use of present models. Inspection of *S*- and *R*-complexes of any of the inhibitors with any of the two enzymes, reveals that in the case of the *S*-enantiomer, when the carboxylate moiety of the ligand faces residue Arg^{120}, the methyl group faces a small hydrophobic pocket near Leu^{531}. In contrast, in all the *R*-enantiomers complexes the methyl group experiences a steric clash with Ile/Val^{523} resulting in a steric of ligand–enzyme interaction.

Further inspection of the COX active site suggests that, in addition to the docking orientation described above for this family of inhibitors, these molecules can also be accommodated inside the active site in a second orientation. In this novel orientation, the molecular axis rests in the direction defined between residues Arg^{120} and Arg^{513}, filling the lateral pocket of the COX active site. There are two initial possible starting docking structures labeled as models 1 and 2, respectively. Taking ketoprofen as a proof of principle, in model 1 the carboxylic moiety rests close to Arg^{513} and the molecule extends towards the mouth of the active site with its ketone group interacting with Tyr^{355}. On the other hand, in model 2 the carboxylate rests close to Arg^{120} and the phenyl ring penetrates into the side pocket. A hydrogen bond between the ketone and Tyr^{355} is also present. Optimization of the proposed complexes shows that ketoprofen remains stable in model 2 (see Fig. 5) in the two isozymes, exhibiting interactions between the carboxylate group and Arg^{120}, the ketone group with Tyr^{355} and phenyl ring with Phe^{518}. In the case of model 1, although the inhibitor is well accommodated in the side pocket, the interaction with Arg^{513} is not possible, and the ligand shows an interaction with Tyr^{355} and His^{90} instead. Interestingly, in COX-1 the inhibitor is shifted from the side pocket due to an steric clash between of the more voluminous Ile^{523} (Val in COX-2) and the methyl group of the acetic acid moiety. In contrast, in COX-2 this methyl group is placed in a hydrophobic pocket surrounded by Gly^{519}, Ala^{516}, Phe^{518} and Val^{523}.

3.2. Acetic acid derivatives: zomepirac

Zomepirac was selected as a representative inhibitor of the acetic acid family of NSAIDs. The molecule (see Fig. 3) consist of a substituted pyrrole ring that serves as scaffold to attach an acetyl moiety in position 5, two methyl groups in positions 1 and 3, respectively, and a 4-chlorobenzoyl group in position 2.

Due to steric hindrance the molecule adopts a conformation where the planes of the two aromatic moieties are perpendicular to each other. Since the structure of the ligand exhibits the same key structural features of the phenylacetic inhibitors, it was considered that the molecule docks into the COX active site in a similar orientation as flubiprofen. Consequently, docking of the compound was guided by the crystal structures of the flubiprofen complexes, that were used as template. Accordingly, the molecule was placed in the active site with the ketone group facing the Ser^{530}

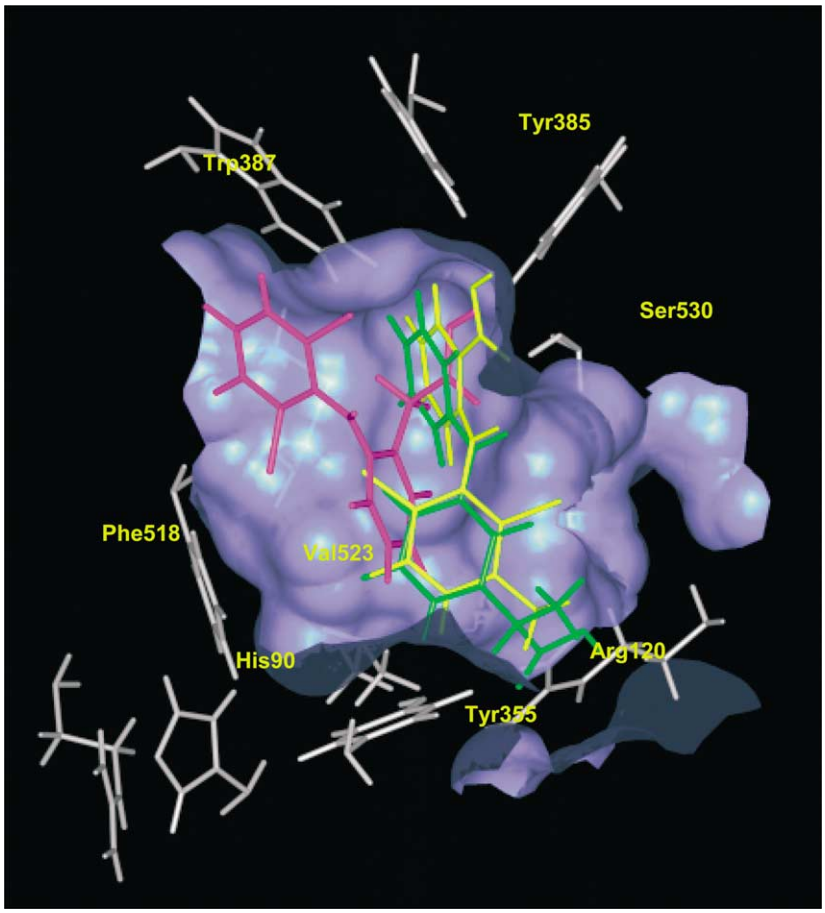

Fig. 4. Superposition of the optimized structures of ketoprofen (in green), meclofenamic acid (yellow) and diclofenac (magenta) bound onto the binding site of COX-2, whose inner surface is displayed in blue. Side chains of key residues are also shown.

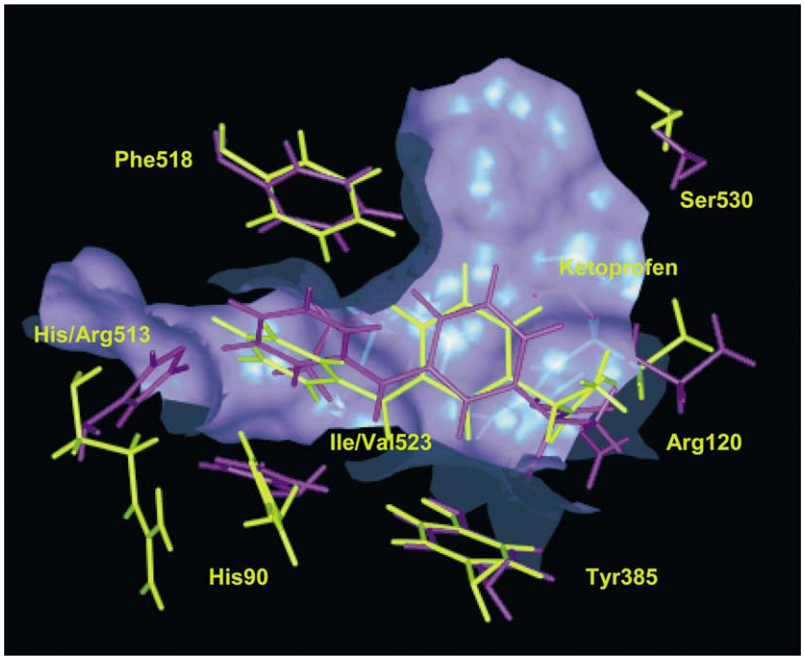

Fig. 5. Superposition of the optimized structures of ketoprofen bound according to model 2 to each of the two isozymes. Docking onto COX-1 is shown in yellow, and onto COX-2 in magenta. The inner surface of the binding pocket is shown in blue.

side chain, the carboxylate group placed in the vicinity of Arg^{120} and the phenyl ring placed inside the aromatic pocket near Tyr^{385}. After the minimization process, the two latter interactions remained, whereas the interaction between the ketone group and the Ser^{530} side chain was lost in all the attempts undertaken. Analysis of the final structure reveals the key role played by the two methyl groups in the docking process. Indeed, after optimization the two methyl groups rest on favorable hydrophobic regions, surrounded by residues Leu^{353}, Leu^{351} and Val^{349}. Accordingly, the two methyl groups of zomepirac play a dual role in explaining the docking process of the ligand. On the one hand, they constrain the relative orientation of the 4-chlorobenzoyl and pyrrole rings, and on the other, force the orientation of the ligand inside the active site, in such a way that the ketone group remains distant of the Ser^{530} side chain. This two features explain the lower affinity exhibited by the compound compared to ketoprofen.

3.3. Fenamic acid derivatives: meclofenamic acid

Ligands of this family of inhibitors consist of a 2-aminobenzoic acid moiety with an aromatic ring attached in *ortho*. Specifically, meclofenamic acid exhibits an aromatic ring with two bulky chlorine substituents in positions 2 and 6, in addition to a methyl group in position 3. The two chlorines flank the amino group that links the aromatic ring to the 2-aminobenzoic acid moiety.

Site directed mutagenesis studies identified different amino acids playing a key role in meclofenamic acid binding. Thus, mutation of Ser^{530} to Met^{530} [26] leads to a loss of inhibition of the ligand, however, mutation of Ser^{530} to Ala^{530} only slightly affects its binding affinity [29]. Furthermore, mutation of Arg^{120} to Glu^{120} in COX-2 does not affect binding of the inhibitor [25]. These results clearly suggest that the carboxylate moiety of the inhibitor does not interact directly with the side chain of Arg^{120}.

In order to identify prospective points in the active site suitable to accommodate the carboxylate moiety of the inhibitor, interaction maps using a carbonyl probe were computed by means of the GRID program [34,35]. These calculations identified two hot spots suitable to provide such a favorable interaction: (i) a region between residues Tyr^{355} and Ser^{353} and (ii) a region located in the neighborhood of Ser^{530} and Tyr^{385} (see Fig. 6). In order to identify regions for suitable interaction regions where the inhibitor aromatic rings could be accommodated in the active site additional GRID calculations using an aromatic probe were also computed. Fig. 6 shows the results of these calculations that were subsequently used to generate different positions for ligand docking purposes.

When the ligand was placed in the active site with the carboxylate moiety facing the region between Tyr^{355} and Ser^{353}, no stable docking was found after minimization, even though different starting geometries were tried. In contrast, when the acid moiety was placed facing the region between Ser^{530} and Tyr^{385} a stable complex could be observed during the minimization process. In its orientation, the inhibitor carboxylate group attains a conformation that is stabilized by a hydrogen bond between the amine nitrogen and the carbonyl oxygen of the acid (yellow ligand in Fig. 4), similar to the unproductive X-ray crystal structure of arachidonic acid bound to COX-2 [39].

The model described above provides an explanation of the slight decrease of affinity produced by the mutation of Ser^{530} to Ala^{530}. Specifically, it can be explained assuming that there is no specific interaction between the ligand and the Ser^{530} side chain. In this case, since the volume of the two side chains is similar the mutation does not create any additional steric hindrance and the affinity is expected to be similar. The loss of the proton donor capability is compensated by the complementary role played by the pair Tyr^{385} and Ser^{530} in the interaction with the inhibitor carboxylate moiety. In contrast, the mutation Ser^{530} to Met^{530} produces a dramatic drop in affinity. This result can be explained on the basis of a steric hindrance produced by the larger volume of the methionine side chain that prevents binding of the ligand. It is worth noting that this effect is not observed in other inhibitors like ketoprofen or indomethacin, due to their differential docking orientation.

3.4. 2-Aminophenylacetic derivatives: diclofenac

Ligands of this family of inhibitors consist of a 2-aminophenylacetic acid scaffold, with an aromatic ring attached in ortho. These structures differ slightly compared to the fenamates, exhibiting an extra methylene unit between the carboxylate group and the aromatic ring. Specifically, diclofenac exhibits an aromatic ring with two bulky chlorine substituents in positions 2 and 6, flanking the amino group that links the two aromatic rings (see Fig. 3).

Like meclofenamic acid, binding of diclofenac is not altered by the mutation of Arg^{120} to Glu^{120} [25], but is dramatically affected by mutation of Ser^{530} to Met^{530} [26]. Unfortunately, there are no experimental results available for the Ser^{530} to Ala^{530} mutation.

In order to explore possible docking orientations of the ligand into the COX binding site, GRID interaction maps using both a carbonyl and a aromatic, respectively, were used as guide (see Fig. 6). Like in the previous case, starting structures were constructed by placing the carboxylate moiety of the inhibitor at a close distance of the pairs Tyr^{355}/Ser^{353} or Tyr^{385}/Ser^{530}. Docking proceeded in a similar fashion as described above for meclofenamic acid. Geometry optimization of the complexes revealed that residues Tyr^{355}/Ser^{353} are not accessible to the inhibitor acid moiety. In contrast, diclofenac appears to be able to interact with the pair Tyr^{385}/Ser^{530} in two different conformations. In one of the conformations, the inhibitor exhibits a similar geometry to meclofenamic acid, where the dichlorophenyl ring is extended through the hydrophobic channel of the active site. On the other conformation, the phenyl ring rests in an

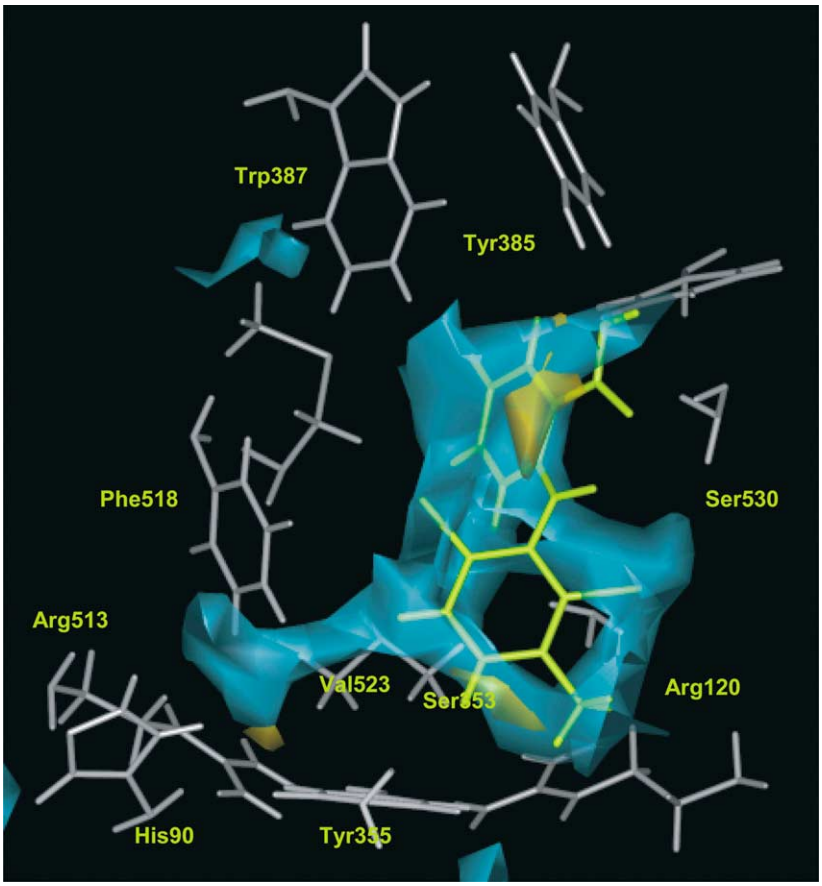

Fig. 6. GRID interaction energy maps computed with a carbonyl probe (in light green) and with an aromatic probe (in orange) on the COX-2 binding site. A starting docking structure of meclofenamic acid (in yellow) is also shown.

aromatic pocket between residues Trp^{387} and Leu^{352}, as shown in Fig. 4. No clear preference between the two complexes can be assessed so far, since both conformations exhibit similar interactions with the receptor and both are consistent with the mutagenesis results and with the GRID calculations.

3.5. Indolacetic acid derivatives: indomethacin

The structure of indomethacin consists of an 1H-indole-3-acetic acid scaffold substituted with a *p*-chlorobenzoyl moiety in position 1, a methyl and an acetyl groups in positions 2 and 3, respectively, and a methoxyl group in position 5. The molecule exhibits two conformations, denoted as *cis* and *trans*, that are interchangeable through a 180° rotation around the amide bond, and evidenced in its crystal structure of the isolated molecule [39].

The crystal structure of the iodine analog of indomethacin bound to COX-1, could not be solved at a higher resolution than 4.5 Å [40]. At this resolution only the electron density of the iodine atom of indomethacin could unambiguously be located, showing that the iodophenyl moiety binds at the end of the long channel near the Tyr^{385} as found for phenyl acetic acid family of inhibitors. The rest of the molecule could be fitted inside the COX binding site in the two possible *cis*- and *trans*-conformations. In contrast, the crystal structure of indomethacin bound to COX-2 at 2.9 Å resolution solved by a different group shows the *cis*-conformation [16].

According to the previous discussion, both the *cis*- and the *trans*-conformations of indomethacin were considered as starting structures for docking studies. Both conformations can be docked into the binding pocket of both isozymes with the carboxylate moiety in the vicinity of Arg^{120}, the ketone group facing Ser^{530} side chain and the *p*-chlorophenyl ring accommodated in the aromatic pocket near Tyr^{385}. However, whereas in the *cis*-conformer the indole is surrounded by Val^{349}, Ser^{353} and Leu^{352}, in the *trans*-isomer this moiety lies next to Val^{349}, Ala^{527}, Leu^{531}.

The superposition of the final structures of the two isomers bound to COX-1, after the optimization process are depicted pictorially in Fig. 7. Analysis of the two complexes of COX-1 reveals that all the interactions of the starting complex in both isozymes are preserved during the minimization process. However, in the resulting *trans*-COX-1 complex, the guanidinium and carboxylate moieties lie in different planes as had already found in the crystal structure [40]. In contrast, in the case of the COX-2 complexes, whereas the *cis*-isomer maintains all the interactions of the starting structure, in the

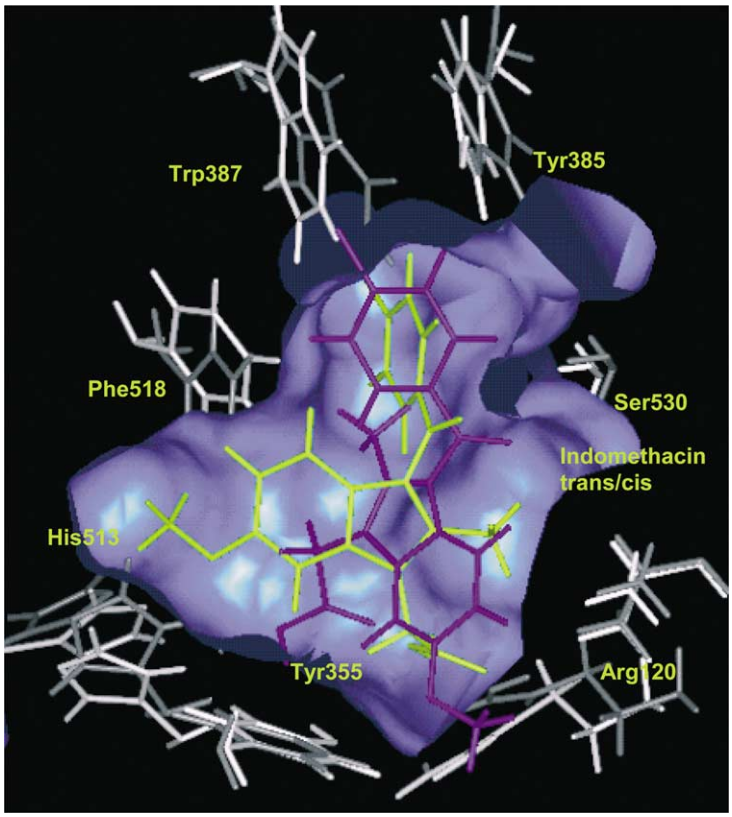

Fig. 7. Superposition of the structures of indomethacin in its *trans*- (in blue) and *cis*-conformations (in yellow) bound into the binding site of COX-1, whose inner surface is displayed in blue.

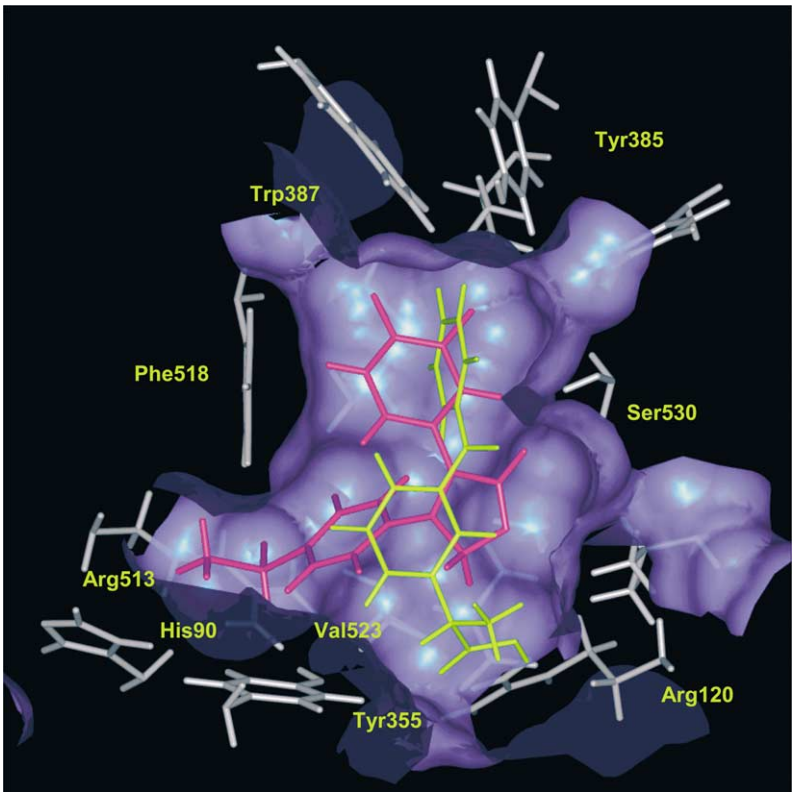

Fig. 8. Structure of rofecoxib (in magenta) and ketoprofen (in yellow) docked into the binding site of COX-2, whose inner surface is shown in blue.

trans-isomer, the interaction between the ketone group and the Ser^{530} side chain is lost, although in both complexes the guanidinium and carboxylate moieties remain in the same plane, similarly to the structures of the *cis*-COX-1 complex. These results suggest that the *trans*-conformation exhibits lower affinity than the *cis*-isomer for both isozymes. Specifically, in COX-2 the reason of the lower affinity appears to be the loss of the interaction between Ser^{530} side chain and the carbonyl moiety. In contrast, in COX-1 the lower affinity is due to the poor interaction between the carboxylate and the guanidinium moieties appears to be detrimental for its binding capacity.

These results agree with the X-ray diffraction structures reported. In the case of COX-1, although the structure could not be unambiguously refined to a higher resolution than 4.5 Å, based on different structural arguments and the inhibitory activity of the two geometric isomers of the indomethacin analog ((*Z*/*E*)-1-(*p*-chlorobenzylidene)-2-methyl-5-methoxyindenylacetic acid (also known as MK-715) [41], the authors proposed the *cis*-conformation as the most favorable complex. On the other hand, in the case of the COX-2 complex the *cis*-isomer is the only structure found in the crystals, supporting the hypothesis of present models.

3.6. Tricyclic derivatives: rofecoxib

The structure of rofecoxib consist of a central five membered lactone ring scaffold with a 4-(methylsulphonyl)phenyl moiety and by a phenyl ring attached to it (see Fig. 3). This tricyclic structure is common to many high affinity selective COX-2 ligands.

3.6.1. Docking of rofecoxib into the active site of COX-2

No crystal structure of the rofecoxib–COX complex is available in the literature so far. The closest structure available at present, is the structure of the tricyclic ligand SC-558 complexed in COX-2 [16], that can be used as guide for the present docking studies. In this structure, the phenyl ring of the inhibitor fills the upper aromatic pocket and the phenylsulphonamide moiety occupies the side pocket, with the sulfonamide moiety resting close to Arg^{513}. However, since SC-558 lacks the furanone moiety of rofecoxib, which could be responsible of extra interactions with different residues of the active site, different starting structures of the inhibitor/enzyme complex were investigated.

Site directed mutagenesis studies suggest that Arg^{513} is a key residue for the affinity of the tricyclic inhibitors to COX, whereas Arg^{120} does not play any significant role in this regard [20,24,25]. The crystal structure of SC-558 reveals that the interaction of the ligand with Arg^{513} is mediated through the sulphone moiety. GRID interaction energy calculations [34,35] performed with a carbonyl oxygen and a ester oxygen probes, respectively, indicate that both Ser^{530} and Arg^{120} are possible binding points of the furanone moiety of the ligand. Accordingly, two different initial structures were tried: (1) in model 1, the ester oxygen of the furanone was placed in the vicinity of the Arg^{120} side chain; (2) in model 2, the carbonyl oxygen was placed close to the side chain of Ser^{530} to consider the possible formation of hydrogen bond between the carbonyl oxygen and the side chain of Ser^{530}. In both complexes, the sulphone was placed in the vicinity of the Arg^{513} side chain. The energy optimization process of the two complexes revealed model 2 to be more favorable, due to good accommodation of the aromatic ring in the hydrophobic pocket, as can be seen in Fig. 8.

3.6.2. Docking of rofecoxib in the active site of COX-1

Docking of rofecoxib into the active site of COX-1 was performed using the previously refined rofecoxib–COX-2 complex as template. Accordingly, the different key interactions between the ligand and the enzyme were conserved in the starting structures: (i) the sulphone moiety was placed in the side pocket, facing His^{513}, the phenyl ring was placed in the upper aromatic pocket and carbonyl moiety was placed close to Ser^{530} side chain. After energy minimization, the inhibitor remained in the same position, suggesting that the steric hindrance due to the substitution Ile/Val^{523} is not enough for preventing the binding of the ligand to COX-1. The superposition of COX-1 and -2 models reveal that the sulphone moiety can be accommodated in COX-1 with only a small deviation in regard its starting position, due to the displacement of the helix fragment corresponding to residues 516–521 and the movement of side chain of Phe^{518}, showing that the side pocket is flexible enough to accommodate the ligand.

4. Discussion

Present models combine the structural information available of different NSAID bound to the COX binding site of the two COX isozymes, together with the reported results of key mutations on the enzymes, that modify or not the biological profile of different inhibitors. The analysis of these models reveals differential binding modes among different families of inhibitors and permits to sketch the main features responsible for ligand binding and selectivity for the different isoforms of the enzyme.

The results of the present work suggest that there are three key ligand–enzyme interactions, responsible for non-selective COX inhibition: (i) a strong hydrogen bond between a ligand carboxylate moiety and the side chain of Arg^{120} or between the pair Tyr^{385}/Ser^{530}; (ii) a hydrogen bond between a ligand accepting group that binds through a hydrogen bond with the Ser^{530} side chain and (iii) an interaction between an aromatic ring that accommodates in a hydrophobic pocket where Tyr^{385} is located. The results of the present models also reveal the importance of the spatial arrangement of the required structural features in the structure of the inhibitors. Ligands are basically planar and the different key moieties, can adequately be arranged by using a planar scaffold that acts as spacer. In most of the

non-selective ligands, this spacer is a six-membered ring, although zomepirac and indomethacin demonstrate that this is not a requirement. Moieties attached to the central scaffold are required to fulfil certain structural features for an increased inhibitory profile. Thus, the carboxyl moiety can be in *ortho*, *meta* or *para* positions in regard to the other aromatic moiety of the molecule. Interestingly, this appears to make a difference in the binding mode of the ligands. In the case the carboxyl moiety is in *ortho*, ligands appear in a bound orientation such that the carboxyl moiety interacts with Tyr^{385}. In contrast when the carboxyl moiety is in *meta* or *para*, the ligand binds in such a way that the carboxyl moiety forms a strong hydrogen bond with the Arg^{120} side chain. This feature was observed in the docking studies of meclofenamic acid and diclofenac, and suggests that these families of NSAIDs do not fulfill the same pharmacophore requirements as the rest of non-selective inhibitors described in the present work. First, the lack of effect on affinity of the mutation Arg^{120} to Glu^{120} [25], clearly suggests that these molecules bind in a different fashion than the arylacetic acid derivatives. Moreover, the mutation of Ser^{530} to Ala^{530} [29] and to Met^{530} [26] clearly reveal that these two inhibitors are much sensitive to the presence of bulky residues in the region close to Ser^{530} than other NSAIDs. These results clearly indicate that diclofenac and meclofenamic acid binding modes require to occupy a larger region in the neighborhood of Ser^{530} that is not required by other NSAIDs. Based on the models constructed in the present work, the binding mode of these two inhibitors can be explained on the basis of the hydrogen bonding interaction between the Tyr^{385} side chain and the carboxylate moiety of the ligands. The feasibility of this binding orientation is supported by the recent X-ray diffraction structure of the arachidonic acid bound to COX-2 [38], where arachidonic acid adopts a conformation that permits its carboxylate moiety to lay close to the side chains of Tyr^{385} and Ser^{530} in a similar way as meclofenamic acid and diclofenac do.

Models also reveal important structural features regarding the characteristics of the different moieties attached to the central scaffold. Thus, the relative spatial position of the planes defined by the spacer and the aromatic ring is an important feature to be considered. Models show that the angle between the two planes should be around 30–40° for an improved ligand–enzyme interaction. This feature permits to explain the reduced affinity exhibited by carprofen. Another feature that modulates affinity is the proton accepting capability of the group that links the spacer and the aromatic ring. The carbonyl appears to be the most suitable, being the inhibitory potency lower for poorer proton accepting groups. Present models suggest this feature to be the reason for the reduced inhibitory potency of fenoprofen. Finally, a methyl group near the carboxyl moiety with a stereoselectivity requirement appears to improve ligand affinity. Thus, when *R*-inhibitors are docked in the active site with the carboxylate moiety resting close to Arg^{120}, exhibit an steric hindrance between the methyl group and the side chain of Ile/Val^{523}. In contrast, *S*-inhibitors dispose their methyl groups in a small hydrophobic pocket close to Leu^{531}.

COX selectivity can be pursued by designing ligands targeted to interact with the non-conserved residues of the two enzymes. Tricyclic inhibitors are designed to occupy the additional side pocket that extends off the COX binding pocket. These ligands are larger than traditional NSAIDs and take advantage of a polar interaction with the non-conserved residue Arg^{513} (His^{513} in COX-1), that rests at the bottom of this lateral pocket of COX-2. Furthermore, in addition, to this difference there is a non-conserved residue: Val^{523} in COX-2 and Ile^{523} in COX-1 strategically located on the confluence of the side pocket and COX binding site. Both residues Arg^{513} and Val^{523} have been demonstrated to be important for COX-2 selective inhibitor binding [24]. The role of the first residue can be understood from static models of rofecoxib, since it provides a polar interaction to the ligand. However, the role of Val^{523} cannot clearly be elucidated from a static model. Indeed, being more voluminous in COX-1 produces a steric hindrance that difficulties binding of the ligands to the lateral pocket of COX-1, as recently identified by free energy perturbation calculations [42,43]. However, static models may not represent accurately the binding of these inhibitors. Present results suggest that the lateral pocket in COX-1 appears to be flexible enough to accommodate ligands at this site, as demonstrated by the docking of ketoprofen and rofecoxib in COX-1. It is possible that in addition to steric reasons, Val^{523} acts as a modulator of the kinetic/dynamic behavior of the ligands. Indeed, tricyclic compounds are time dependent (irreversible) inhibitors of COX-2, and they also exhibit a lower, but time independent (reversible) inhibition behavior in COX-1 [24]. The mutation Val^{513} to Ile^{513} in COX-2 changes the time dependent behavior of different tricyclic inhibitors to a time independent behavior, and preserving part of their inhibitory profile [22]. Extensive molecular modeling studies are required to further understand the dynamics of the inhibition process and the structural rearrangements associated with these two types of inhibition.

5. Conclusions

Systematic docking of selective and non selective ligands in the active site of both isozymes was undertaken, using the available structural information together with site directed mutagenesis results reported in the literature. Models constructed show different features regarding the characterization of key structural motifs of ligands involved in COX inhibition. Several structural features are considered to be important for efficient COX inhibition: (i) a carboxylate moiety that interacts with the Arg^{120} side chain; (ii) a carbonyl moiety that interacts via a hydrogen bond with the side chain of Ser^{530} and (iii) a distal aromatic ring filling a hydrophobic pocket beneath the Tyr^{385} side chain. These three moieties need to be attached to a scaffold that

most commonly is a six-membered ring. However, present results evidence a differential binding mode of the ligand, depending on the relative position of the carboxyl and aromatic moieties on the scaffold. This observation could be drawn after the analysis of the models of meclofenamic acid or diclofenac when compared to those of ketoprofen or zomepirac This result conciliate and is supported by different site directed mutagenesis studies reported in the literature. Present models also explore the possibility that non-selective ligands bind also in a different orientation as demonstrated for ketoprofen. This binding orientation could be interpreted as an intermediate mode of binding for the ligands in their way to the COX binding pocket.

Selective COX-2 tricyclic inhibitor rofecoxib show a similar disposition when docked into the active site of both isoenzymes. This is possible through a displacement of the sulphone moiety and an induced fit of the helix that maintains Phe^{518} at the same time in COX-2.

Acknowledgements

The authors wish to thank the helpful comments of an anonymous referee to enrich the present manuscript. CESCA is gratefully acknowledged for a generous allocation of computer time through a grant to the project *Molecular Engineering*. O. Llorens wishes to thank the *Generalitat de Catalunya* for a fellowship to undertake this work.

References

[1] R.M. Smith, D.L. DeWitt, R.M. Garavito, CYCLOOXYGENASES: structural, cellular, and molecular biology, Ann. Rev. Biochem. 69 (2000) 145–182.
[2] H. Herschman, Function and regulation of prostaglandin synthase 2, Adv. Exp. Med. Biol. 469 (1999) 3–8.
[3] D.E. Griswold, J.L. Adams, Constitutive cyclooxygenase (COX-1) and inducible cyclooxygenase (COX-2): rationale for selective inhibition and progress to date, Med. Res. Rev. 16 (1996) 181–206.
[4] D. Munroe, C.Y. Lau, Turning down the heat: new routes to inhibition of inflammatory signaling by prostaglandin H2 synthases, Chem. Biol. 2 (1995) 343–350.
[5] H. Herschman, Prostaglandin synthase 2, Biochim. Biophys. Acta. 1299 (1996) 125–140.
[6] K. Seibert, Y. Zhang, K. Leahy, S. Hauser, J. Masferrrer, W. Perkins, L. Lee, P. Isakson, Pharmacological and biochemical demonstration of the role of cyclooxygenase 2 in inflammation and pain, Proc. Natl. Acad. Sci. U.S.A. 91 (1994) 12013–12017.
[7] G.P. O'Neill, A.W. Ford-Hutchinson, Expression of mRNA for cyclooxygenase-1 and -2 in human tissues, FEBS Lett. 330 (1993) 156–160.
[8] S. Kargman, S. Charleson, M. Cartwright, J. Frank, D. Riendeau, J. Mancini, J. Evans, G. O'Neill, Characterization of prostaglandin G/H synthase 1 and 2 in rat, dog, monkey, and human gastrointestinal tracts, Gastroenterology 111 (1996) 445–454.
[9] J. Vane, Towards a better aspirin, Nature 367 (1994) 215–216.
[10] J.J. Talley, Selective inhibitors of cyclooxyganase-2, Exp. Opin. Ther. Patents 7 (1997) 55–62.
[11] L.A. Sorbera, P.A. Leeson, J. Castañer, Rofecoxib, Drugs of the future 23 (1998) 1287–1296.
[12] T.J. Schnitzer, Cyclooxygenase-2-specific inhibitors: are they safe? Am. J. Med. 110 (Suppl. 1) (2001) S46–S49.
[13] D. Picot, P.J. Loll, R.M. Garavito, The X-ray crystal structure of the membrane protein prostaglandin H_2 synthase-1, Nature 367 (1994) 243–249.
[14] P.L. DeWitt, Cox-2-selective inhibitors: the new super aspirins, Mol. Pharmacol. 55 (1999) 625–631.
[15] C. Luong, A. Miller, J. Barnett, J. Chow, C. Ramesha, M. Browner, Flexibility of the NSAID binding site in the structure of human cyclooxygenase-2, Nat. Struct. Biol. 3 (1996) 927–933.
[16] R.G. Kurumball, A.M. Stevens, J.K. Gierse, J.J. McDonald, R.A. Stegeman, J.Y. Pak, D. Gildehaus, J.M. Miyashiro, T.D. Penning, K. Seibert, P.C. Isakson, W.C. Stallings, Structural basis for selective inhibition of cyclooxyganase-2 by anti-inflammatory agents, Nature 384 (1996) 644–648.
[17] B.S. Selinsky, K. Gupta, C.T. Sharkey, P.J. Loll, Structural analysis of NSAID binding by prostaglandin H2 synthase: time-dependent and time-independent inhibitors elicit identical enzyme conformations, Biochemistry 40 (2001) 5172–5180.
[18] P.J. Loll, Structure of prostaglandin H2 synthase-1 (COX-1) and its NSAID binding sites, in: N. Bazan, J. Botting, J. Vane (Eds.), New Targets in Inflammation, Inhibitors of COX-2 or Adhesion Molecules, 1996, pp. 13–21.
[19] M. Filizola, J.J. Perez, A. Palomer, D. Mauleon, Comparative molecular modeling study of the three-dimensional structures of prostaglandin endoperoxide H2 synthase 1 and 2 (COX-1 and COX-2), J. Mol. Graph. Model. 15 (1997) 290–300.
[20] J.A. Mancini, D. Rindeau, J.-P. Falgueyret, P.J. Vickers, G.P. O'Neill, Arginine 120 of prostaglandin G/H synthase-1 is required for the inhibition by non-steroideal anti-inflammatory drugs containing a carboxylic acid moiety, J. Biol. Chem. 270 (1995) 29372–29377.
[21] J.K. Gierse, J.J. McDonald, S.D. Hauser, S.H. Rangwala, C.M. Koboldt, K. Seibert, A single amino acid difference between cyclooxyganase-1 (COX-1) and –2 (COX-2) reverses the selectivity of COX-2 specific inhibitors, J. Biol. Chem. 271 (1996) 15810–15814.
[22] Q. Guo, L.-H. Wang, K.-H. Ruan, J. Kulmacz, Role of Val^{509} in time-dependent inhibition of human prostaglandin H synthase-2 cyclooxygenase activity by isoform-selective agents, J. Biol. Chem. 271 (1996) 19134–19139.
[23] D.K. Bhattacharyya, M. Lecomte, C.J. Rieke, R.M. Garavito, W.L. Smith, Involvement of arginine 120, glutamate 524 and tyrosine 355 in the binding of arachidonate and 2-phenylpropionic acid inhibitors to the cyclooxygenase active site of ovine prostaglandin endoperoxide H synthase-1, J. Biol. Chem. 271 (1996) 2179–2184.
[24] E. Wong, C. Bayly, H.L. Watermann, D. Riendeau, J.A. Mancini, Conversion of prostaglandin G/H synthase-1 into an enzyme sensitive to PGHS-2 selective inhibitors by a double $His^{513} \rightarrow$ Arg and $Ile^{523} \rightarrow$ Val mutation, J. Biol. Chem. 272 (1997) 9280–9286.
[25] G.M. Greig, A.F. Donna, J.-P. Falgueyret, M. Ouellet, M.D. Percival, P. Roy, C. Boily, J.A. Mancini, G.P. O'Neill, The interaction of arginine 106 of human prostaglandin G/H synthase-2 with inhibitors is not a universal component of inhibition mediated by non-steroidal anti-inflammatory drugs, Mol. Pharm. 52 (1997) 829–838.
[26] J.A. Mancini, P.J. Vickers, G.P. O'Neill, C. Boily, J.-P. Falgueyret, D. Rindeau, Altered sensitivity of aspirin-acetylated prostaglandin G/H synthase-2 to inhibition by non-steroidal anti-inflammatory drugs, Mol. Pharm. 51 (1997) 52–60.
[27] O.-Y. So, L.E. Scarafia, A.Y. Mak, O.H. Callan, D.C. Swinney, The dynamics of prostaglandin H synthases, J. Biol. Chem. 273 (1998) 5801–5807.
[28] C.J. Rieke, A.N. Mulichak, R.M. Garavito, W.L. Smith, The role of arginine 120 of human prostaglandin endoperoxide H synthase-2 in the interaction with fatty acid substrates and inhibitors, J. Biol. Chem. 274 (1999) 17109–17114.
[29] A.S. Kalgutkar, B.C. Crews, S.W. Rowlinson, A.B. Marnett, K.R. Kozak, R.P. Remmel, L.J. Marnett, Biochemically-based design of cyclooxygenase-2 (COX-2) inhibitors: facile conversion of

non-steroidal anti-inflammatory drugs to potent and highly selective COX-2 inhibitors, Proc. Natl. Acad. Sci. U.S.A. 97 (2000) 925–930.
[30] H.M. Berman, J. Westbrook, Z. Feng, G. Gillard, T.N. Bhat, H. Weissig, I.N. Shindyalov, P.E. Bourne, The Protein Data Bank, Nucl. Acids Res. 28 (2000) 235–242.
[31] D.A. Pearlman, D.A. Case, J.C. Caldwell, G.L. Seibel, V.C. Singh, P. Weiner, P.A. Kollman, AMBER, University of California, San Francisco, 1991.
[32] S.J. Weiner, P.A. Kollman, D.A. Case, U.Ch. Singh, C. Ghio, G. Alagona, S. Profeta, P. Weiner, A new force field for molecular mechanical simulation of nucleic acids and proteins, J. Am. Chem. Soc. 106 (1984) 765–784.
[33] M.J. Frisch, G.W. Trucks, H.B. Schlegel, P.M.W. Gill, B.G. Johnson, M.A. Robb, J.R. Cheesman, T. Keith, G.A. Petersson, J.A. Montgomery, K. Raghavachari, M.A. Al-Laham, V.G. Zakrzewski, J.V. Ortiz, J.B. Foresman, C.Y. Peng, P.Y. Ayala, W. Chen, M.W. Wong, J.L. Andres, E.S. Replogle, R. Gomperts, R.L. Martin, J. Fox, J.S. Binkley, D.J. Defrees, J. Baker, J.J.P. Stewart, M. Head-Gordon, C. Gonzales, J.A. Pople, GAUSSIAN94, revision B.2, Gaussian Inc., Pittsburg, Pennsylvania, 1995.
[34] P.J. Goodford, A computational procedure for determining energetically favorable binding sites on biologically important macromolecules, J. Med. Chem. 28 (1985) 849–857.
[35] GRID Version 17.0, Molecular Discovery Ltd., Oxford, 1998.
[36] InsightII, Molecular Simulations, San Diego, CA, 1998.
[37] F. Cabre, A. Carabaza, unpublished results.
[38] J.R. Kiefer, J.L. Pawlitz, K.T. Moreland, R.A. Stageman, W.F. Hood, J.K. Gierse, A.M. Stevens, D.C. Goodwin, S.W. Rowilson, L.J. Marnett, W.C. Stallings, R.G. Kurumbail, Structural insights into the stereochemistry of the cyclooxygenase reaction, Nature 405 (2000) 97–101.
[39] P.J. Lloll, C.J. Carrell, H.C. Carrell, R.M. Garavito, 1-(4-iodobenzoyl)-5-methoxy-2-methyl-3-indoleacetic acid, an iodinated indomethacin analog, Acta. Crystallogr. C. 52 (1996) 455–457.
[40] P.J. Loll, D. Picot, O. Ekabo, R.M. Garavito, Synthesis and use of iodinated non-steroidal anti-inflammatory drug analogs as crystallographic probes of the prostaglandin H2 synthase cyclooxygenase active site, Biochemistry 35 (1996) 7330–7340.
[41] K. Hoogsteen, N.R. Trenner, The structure and conformation of the *cis*- and *trans*-isomers of 1-(*p*-chlorobenzylidene)-2-methyl-5-methoxyindenylacetic acid, J. Org. Chem. 35 (1970) 521–523.
[42] M.L.P. Price, W.L. Jorgensen, Analysis of binding affinities for celecoxib analogues with COX-1 and COX-2 from combined docking and Monte Carlo simulations and insight into the COX-2/COX-1 selectivity, J. Am. Chem. Soc. 122 (2000) 9455–9466.
[43] M.L.P. Price, W.L. Jorgensen, Rationale for the observed COX-2/COX-1 selectivity of celecoxib from Monte Carlo simulations, Bioorg. Med. Chem. Lett. 11 (2001) 1541–1544.